# Channel Shaping Using Reconfigurable Intelligent Surfaces: From Diagonal to Beyond

Yang Zhao, *Member, IEEE,* Hongyu Li, *Graduate Student Member, IEEE,*
Yijie Mao, *Member, IEEE,* Shanpu Shen, *Member, IEEE,* and Bruno Clerckx, *Fellow, IEEE*

## I. Assumption

We introduce Beyond-Diagonal (BD) Reconfigurable Intelligent Surface (RIS) in Multiple-Input Multiple-Output (MIMO) Point-to-point Channel (PC) and Interference Channel (IC). All proposals are based on assumption of *asymmetric* passive BD RIS, i.e., symmetry constraint $\mathbf{\Theta}_g = \mathbf{\Theta}_g^{\mathsf{T}}$ is relaxed. This is feasible when asymmetric passive components (e.g., ring hybrids and branch-line hybrids) [1] are available. This assumption was also made in Hongyu's papers [2], [3]. For quadratic problems, the proposed algorithms may be extended to symmetric BD RIS by replacing singular value decomposition with Takagi factorization [4].

## II. MIMO-PC

### A. Channel Power Maximization

Consider a BD RIS with $N^{\mathrm{S}}$ elements, which is divided into $G$ groups of equal $L$ elements.

$$\max_{\mathbf{\Theta}} \quad \left\|\mathbf{H}^{\mathrm{D}}+\sum\nolimits_g \mathbf{H}_g^{\mathrm{B}}\mathbf{\Theta}_g\mathbf{H}_g^{\mathrm{F}}\right\|_{\mathrm{F}}^2 \tag{1a}$$

$$\text{s.t.} \quad \mathbf{\Theta}_g^{\mathsf{H}}\mathbf{\Theta}_g=\mathbf{I}, \quad \forall g\in\mathcal{G}\triangleq\{1,...,G\}. \tag{1b}$$

For *symmetric* BD-RIS, the problem has been solved in

- Matteo's paper [5]: SISO and equivalent[1];
- Ignacio's paper [6]: SISO and directless MISO/SIMO.

**Remark 1.** *The difficulty of* (1) *is that the RIS needs to balance the additive (direct-indirect) and multiplicative (forward-backward) eigenspace alignment. Interestingly, it has the same form as the* weighted orthogonal Procrustes problem *[7]:*

$$\min_{\mathbf{\Theta}} \quad \|\mathbf{C}-\mathbf{A}\mathbf{\Theta}\mathbf{B}\|_{\mathrm{F}}^2 \tag{2a}$$

$$\text{s.t.} \quad \mathbf{\Theta}^{\mathsf{H}}\mathbf{\Theta}=\mathbf{I}. \tag{2b}$$

*There exists no trivial solution to* (2)*. One lossy transformation, by moving* $\mathbf{\Theta}$ *to one side [8], formulates a standard orthogonal Procrustes problem:*

$$\min_{\mathbf{\Theta}} \quad \|\mathbf{A}^{\dagger}\mathbf{C}-\mathbf{\Theta}\mathbf{B}\|_{\mathrm{F}}^2 \tag{3a}$$

$$\text{s.t.} \quad \mathbf{\Theta}^{\mathsf{H}}\mathbf{\Theta}=\mathbf{I}. \tag{3b}$$

(3) *has a global optimal solution* $\mathbf{\Theta}^{\star}=\mathbf{U}\mathbf{V}^{\mathsf{H}}$*, where* $\mathbf{U}$ *and* $\mathbf{V}$ *are left and right singular matrix of* $\mathbf{A}^{\dagger}\mathbf{C}\mathbf{B}^{\mathsf{H}}$ *[9]. This low-complexity solution will be compared with the one proposed later.*

[1]Single-stream MIMO with given precoder and combiner.

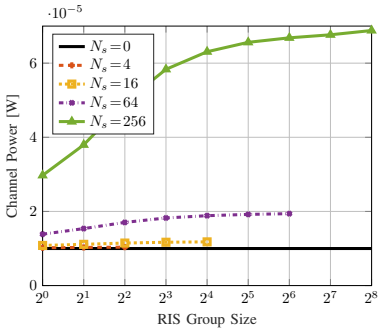


Fig. 1. Average channel power versus RIS elements $N^{\mathrm{S}}$ and group size $L$ for $(N^{\mathrm{T}},N^{\mathrm{R}})=(8,4)$, $(\Lambda^{\mathrm{D}},\Lambda^{\mathrm{F}},\Lambda^{\mathrm{B}})=(65,54,46)$dB.

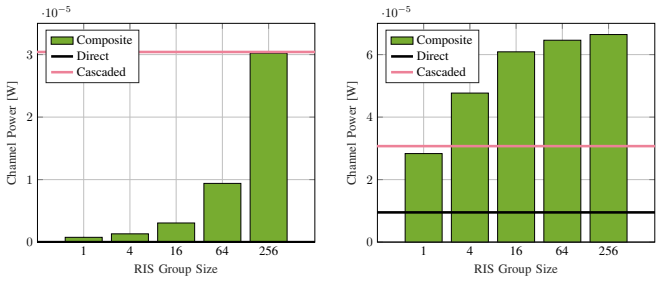


(a) Without Direct Link (b) With Direct Link

Fig. 2. Average channel power versus RIS group size $L$ for $(N^{\mathrm{T}},N^{\mathrm{S}},N^{\mathrm{R}})=(8,256,4)$, $(\Lambda^{\mathrm{D}},\Lambda^{\mathrm{F}},\Lambda^{\mathrm{B}})=(65,54,46)$dB.

Inspired by [10], we propose an iterative algorithm to solve (1). The idea is to successively approximate the quadratic objective with a sequence of affine functions and solve the resulting subproblems in closed form.

**Proposition 1.** *Start from any* $\mathbf{\Theta}^{(0)}$*, the sequence*

$$\mathbf{\Theta}_g^{(r+1)}=\mathbf{U}_g^{(r)}\mathbf{V}_g^{(r)}, \quad \forall g \tag{4}$$

*converges to a stationary point of* (1)*, where* $\mathbf{U}_g^{(r)}$ *and* $\mathbf{V}_g^{(r)}$ *are left and right singular matrix of*

$$\begin{aligned}\mathbf{M}_g^{(r)}=&\mathbf{H}_g^{\mathrm{B}\,\mathsf{H}}\mathbf{H}^{\mathrm{D}}\mathbf{H}_g^{\mathrm{F}\,\mathsf{H}}+\sum_{g'<g}\mathbf{H}_{g'}^{\mathrm{B}\,\mathsf{H}}\mathbf{H}_{g'}^{\mathrm{B}}\mathbf{\Theta}_{g'}^{(r+1)}\mathbf{H}_{g'}^{\mathrm{F}}\mathbf{H}_{g'}^{\mathrm{F}\,\mathsf{H}}\\&+\sum_{g'\geq g}\mathbf{H}_{g'}^{\mathrm{B}\,\mathsf{H}}\mathbf{H}_{g'}^{\mathrm{B}}\mathbf{\Theta}_{g'}^{(r)}\mathbf{H}_{g'}^{\mathrm{F}}\mathbf{H}_{g'}^{\mathrm{F}\,\mathsf{H}}.\end{aligned} \tag{5}$$

*Proof.* To be added. □

Fig. 1 shows that, apart from adding reflecting elements $N^{\mathrm{S}}$, increasing the group size $L$ also improves the channel

power. This behavior is more pronounced for a large RIS. For example, the gain of pairwise connection is 2.8 % for $N^{\mathrm{S}}=16$ and 28 % for $N^{\mathrm{S}}=256$. It implies that the channel shaping capability of BD RIS scales with group size $L$.

Fig. 2b and 2a compare the average channel power without and with direct link. "Cascaded" means the *power product* of the forward and backward channels. We observe that diagonal RIS wastes substantial cascaded power and struggles to align the direct-indirect eigenspace. When the direct link is absent, only 2.6 % of available power is utilized by diagonal RIS while 100 % power is recycled by fully-connected RIS. When the direct link is present, the proposed BD RIS design can balance the direct-indirect and forward-backward eigenspace alignment for an optimal channel boost. It is worth noting that, when $L$ is sufficiently large, the composite channel power surpasses the power sum of direct and cascaded channels, thanks to the constructive *amplitude superposition* of direct and cascaded channels. This again emphasizes the advantage of in-group connection of BD RIS.

### B. Rate Maximization

The problem is formulated w.r.t. precoder (instead of transmit covariance matrix) for reference:

$$\max_{\mathbf{W},\boldsymbol{\Theta}} \quad \operatorname{logdet}\left(\mathbf{I}+\frac{\mathbf{W}^{\mathsf{H}}\mathbf{H}^{\mathsf{H}}\mathbf{H}\mathbf{W}}{\sigma_n^2}\right) \tag{6a}$$

$$\text{s.t.} \quad \|\mathbf{W}\|_{\mathrm{F}}^2 \le P, \tag{6b}$$

$$\boldsymbol{\Theta}_g^{\mathsf{H}}\boldsymbol{\Theta}_g=\mathbf{I}, \quad \forall g. \tag{6c}$$

(6) is jointly non-convex and solved by Alternating Optimization (AO). For a given $\boldsymbol{\Theta}$, the optimal precoder is given by

$$\mathbf{W}^{\star}=\mathbf{V}\mathbf{S}^{\star 1/2}, \tag{7}$$

where $\mathbf{V}$ is right singular matrix of $\mathbf{H}$ and $\mathbf{S}^{\star}$ is a diagonal matrix of the water-filling power allocation. For a given $\mathbf{W}$, we update $\boldsymbol{\Theta}$ by Riemannian Conjugate Gradient (RCG) method along the geodesics [11].

**Remark 2.** *A geodesic refers to the shortest path between two points in a Riemannian manifold. Unitary constraint* (6c) *translates to a Stiefel manifold where the geodesics have simple expressions described by the exponential map [12].*

For general optimization problems with block unitary constraint, the adapted RCG method at iteration $r$ for block $g$ is summarized below, where $f\left(\boldsymbol{\Theta}_g^{(r)}\right)$ is the objective function also evaluated over $\left\{\{\boldsymbol{\Theta}_{g'}^{(r+1)}\}_{g'<g},\{\boldsymbol{\Theta}_{g'}^{(r)}\}_{g'>g}\right\}$.

1) Compute the Euclidean gradient

$$\nabla_g^{\mathrm{E}(r)}=\frac{\partial f\left(\boldsymbol{\Theta}_g^{(r)}\right)}{\partial \boldsymbol{\Theta}_g^{*}}; \tag{8}$$

2) Translate to the Riemannian gradient

$$\nabla_g^{\mathrm{R}(r)}=\nabla_g^{\mathrm{E}(r)}\boldsymbol{\Theta}_g^{(r)\mathsf{H}}-\boldsymbol{\Theta}_g^{(r)}\nabla_g^{\mathrm{E}(r)\mathsf{H}}; \tag{9}$$

3) Determine the weight factor

$$\gamma_g^{(r)}=\frac{\operatorname{tr}\left(\left(\nabla_g^{\mathrm{R}(r)}-\nabla_g^{\mathrm{R}(r-1)}\right)\nabla_g^{\mathrm{R}(r)\mathsf{H}}\right)}{\operatorname{tr}\left(\nabla_g^{\mathrm{R}(r-1)}\nabla_g^{\mathrm{R}(r-1)\mathsf{H}}\right)}; \tag{10}$$

**Algorithm 1:** RCG Method for RIS MIMO-PC Rate Maximization

**Input:** $\mathbf{H}^{\mathrm{D}}$, $\mathbf{H}^{\mathrm{F}}$, $\mathbf{H}^{\mathrm{B}}$, $\mathbf{W}$, $L$, $\sigma_n^2$
**Output:** $\boldsymbol{\Theta}^{\star}$
1: $r\leftarrow 0$, $\boldsymbol{\Theta}^{(0)}$
2: **Repeat**
3: $\quad r\leftarrow r+1$
4: $\quad$ **For** $g\leftarrow 1$ to $G$
5: $\quad\quad \boldsymbol{\Theta}_g^{(r)}\leftarrow$ (14), (9)–(13)
6: $\quad$ **End For**
7: **Until** $|R^{(r)}-R^{(r-1)}|/R^{(r-1)}\le\epsilon$

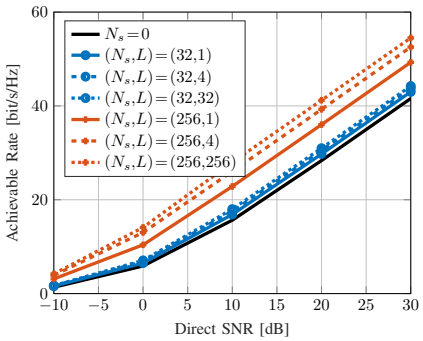


Fig. 3. Average achievable rate versus RIS elements $N^{\mathrm{S}}$ and group size $L$ for $(N^{\mathrm{T}},N^{\mathrm{R}})=(8,4)$, $(\Lambda^{\mathrm{D}},\Lambda^{\mathrm{F}},\Lambda^{\mathrm{B}})=(65,54,46)$dB.

4) Compute the conjugate direction

$$\mathbf{D}_g^{(r)}=\nabla_g^{\mathrm{R}(r)}+\gamma_g^{(r)}\mathbf{D}_g^{(r-1)}; \tag{11}$$

5) Determine the Armijo step size[2]

$$\mu_g^{(r)}=\underset{\mu_g}{\operatorname{argmax}} f\left(\exp\left(\mu_g\mathbf{D}_g^{(r)}\right)\boldsymbol{\Theta}_g^{(r)}\right); \tag{12}$$

6) Perform rotational update along local geodesics

$$\boldsymbol{\Theta}_g^{(r+1)}=\exp\left(\mu_g^{(r)}\mathbf{D}_g^{(r)}\right)\boldsymbol{\Theta}_g^{(r)}. \tag{13}$$

**Remark 3.** *The adapted RCG method leverages the fact that block unitary matrices are closed under multiplication (but not necessarily under addition). Its advantage over universal manifold optimization [13], [14] is trifold:*

- *No retraction is involved;*
- *Lower computational complexity per iteration [12];*
- *Faster convergence thanks appropriate operational space.*

The complex derivative of (6a) w.r.t. RIS block $g$ is

$$\frac{\partial R}{\partial \boldsymbol{\Theta}_g^{*}}=\frac{1}{\sigma_n^2}\mathbf{H}_g^{\mathrm{B}\mathsf{H}}\mathbf{H}\mathbf{W}\left(\mathbf{I}+\frac{\mathbf{W}^{\mathsf{H}}\mathbf{H}^{\mathsf{H}}\mathbf{H}\mathbf{W}}{\sigma_n^2}\right)^{-1}\mathbf{W}^{\mathsf{H}}\mathbf{H}_g^{\mathrm{F}\mathsf{H}}. \tag{14}$$

Algorithm 1 summarizes the adapted RCG method for the RIS rate maximization subproblem.

Fig. 3 illustrates how RIS configuration influences the MIMO PC achievable rate. To ensure a 20 bit/s/Hz transmission, an Signal-to-Noise Ratio (SNR) of 13.5 dB is required for a 8T4R system. This value decreases to 12.5 dB (resp. 8 dB) when 32- (resp. 256-) element diagonal RIS is present. If tetrads can be formed in BD RIS, the SNR can be reduced by another 20 %

[2]To double the step size, simply square the argument instead of recomputing the matrix exponential, i.e., $\exp(2\mu_g\mathbf{D}_g)=\exp^2(\mu_g\mathbf{D}_g)$.

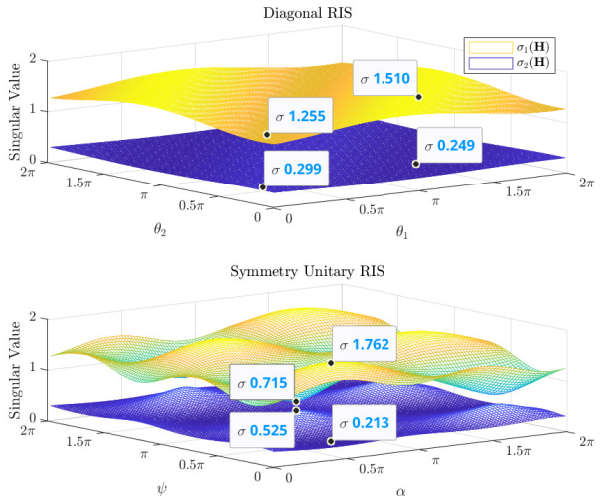


Fig. 4. Channel singular value shaping by diagonal and symmetry unitary RIS for $(N^{\mathrm{T}},N^{\mathrm{S}},N^{\mathrm{R}})=(2,2,2)$ without direct link.

(resp. $44\,\%$). Further increase in $L$ yields a marginal gain and incurs $\mathcal{O}(L^2)$ connections. We thus conclude dyadic or tetradic BD RIS usually strike a good balance between performance and complexity.

### C. Channel Singular Value Redistribution

We first show the channel shaping benefit of BD RIS by a toy example. Consider $(N^{\mathrm{T}},N^{\mathrm{S}},N^{\mathrm{R}})=(2,2,2)$ and assume the direct link is absent. The diagonal RIS is $\mathbf{\Theta}^{\mathrm{D}}=\mathrm{diag}(e^{\jmath\theta_1},e^{\jmath\theta_2})$ while the unitary RIS has 4 independent angular parameters

$$\mathbf{\Theta}^{\mathrm{U}}=e^{\jmath\phi}\begin{bmatrix} e^{\jmath\alpha}\cos\psi & e^{\jmath\beta}\sin\psi \\ -e^{-\jmath\beta}\sin\psi & e^{-\jmath\alpha}\cos\psi \end{bmatrix}. \tag{15}$$

When the direct link is absent, $\phi$ has no impact on the singular value because $\mathrm{sv}(e^{\jmath\phi}\mathbf{A})=\mathrm{sv}(\mathbf{A})$. For a fair comparison, we enforce *symmetry* with $\beta=\pi/2$. Fig. 4 illustrates all possible channel singular values achieved by diagonal and symmetry unitary RIS. Despite using the same number of elements and parameters, BD RIS provides much wider dynamic ranges of $\sigma_1(\mathbf{H})$ and $\sigma_2(\mathbf{H})$ than diagonal RIS. Larger gaps are expected when the symmetry constraint can be relaxed.

We then analyze the channel shaping *capability* of BD RIS under specific setups.

*1) Rank-Deficient Channel:* In rank-deficient channels, BD RIS $\mathbf{\Theta}^{\mathrm{B}}$ cannot achieve a higher Degree of Freedom (DoF) than diagonal RIS $\mathbf{\Theta}^{\mathrm{D}}$. This is because $\mathrm{sv}(\mathbf{\Theta}^{\mathrm{B}})=\mathrm{sv}(\mathbf{\Theta}^{\mathrm{D}})=\mathbf{1}$ and

$$\begin{aligned}\mathrm{rank}(\mathbf{H}) &\le \mathrm{rank}(\mathbf{H}^{\mathrm{D}})+\mathrm{rank}(\mathbf{H}^{\mathrm{B}}\mathbf{\Theta}\mathbf{H}^{\mathrm{F}}) \\ &\le \mathrm{rank}(\mathbf{H}^{\mathrm{D}})+\min\big(\mathrm{rank}(\mathbf{H}^{\mathrm{B}}),\mathrm{rank}(\mathbf{\Theta}),\mathrm{rank}(\mathbf{H}^{\mathrm{F}})\big).\end{aligned} \tag{16}$$

Note BD RIS can still provide a higher indirect SNR as shown in Fig. 1 and 2.

*2) Rank-1 Indirect Channel:* The indirect channel is rank-1 iff the forward or backward channel is rank-1. Let $\mathbf{H}^{\mathrm{F}}=\sigma^{\mathrm{F}}\mathbf{u}^{\mathrm{F}}\mathbf{v}^{\mathrm{F}\mathsf{H}}$ without loss of generality. In this case, the channel Gram matrix can be written as Hermitian-plus-rank-1:

$$\mathbf{G}\triangleq\mathbf{H}\mathbf{H}^{\mathsf{H}}=\mathbf{Y}+\mathbf{z}\mathbf{z}^{\mathsf{H}}, \tag{17}$$

where $\mathbf{Y}\triangleq\mathbf{H}^{\mathrm{D}}(\mathbf{I}-\mathbf{v}^{\mathrm{F}}\mathbf{v}^{\mathrm{F}\mathsf{H}})\mathbf{H}^{\mathrm{D}}=\mathbf{F}\mathbf{F}^{\mathsf{H}}$ and $\mathbf{z}\triangleq\sigma^{\mathrm{F}}\mathbf{H}^{\mathrm{B}}\mathbf{\Theta}\mathbf{u}^{\mathrm{F}}+\mathbf{H}^{\mathrm{D}}\mathbf{v}^{\mathrm{F}}$. Regardless of RIS size and structure[3], its $n$-th $(n\ge 2)$ eigenvalues are bounded by the Cauchy interlacing formula [9]

$$\lambda_1(\mathbf{Y})\ge\lambda_2(\mathbf{G})\ge\lambda_2(\mathbf{Y})\ge\ldots\ge\lambda_{n-1}(\mathbf{Y})\ge\lambda_n(\mathbf{G})\ge\lambda_n(\mathbf{Y}). \tag{18}$$

That is to say, [for sv]

Finally, we characterize the *Pareto front* of channel singular values via optimization approach.

## References


[1] H.-R. Ahn, *Asymmetric Passive Components in Microwave Integrated Circuits*. Wiley, 2006. [Online]. Available: https://books.google.co.uk/books?id=X6WdLbOuSNQC

[2] H. Li, S. Shen, and B. Clerckx, "Beyond diagonal reconfigurable intelligent surfaces: From transmitting and reflecting modes to single-, group-, and fully-connected architectures," *IEEE Transactions on Wireless Communications*, vol. 22, pp. 2311–2324, 4 2023.

[3] ——, "Beyond diagonal reconfigurable intelligent surfaces: A multi-sector mode enabling highly directional full-space wireless coverage," *IEEE Journal on Selected Areas in Communications*, vol. 41, pp. 2446–2460, 8 2023.

[4] R. A. Horn and C. R. Johnson, *Matrix Analysis*. Cambridge University Press, 2012. [Online]. Available: https://books.google.co.uk/books?id=O7sgAwAAQBAJ

[5] M. Nerini, S. Shen, and B. Clerckx, "Closed-form global optimization of beyond diagonal reconfigurable intelligent surfaces," *IEEE Transactions on Wireless Communications*, pp. 1–1, 2023. [Online]. Available: https://ieeexplore.ieee.org/document/10155675/

[6] I. Santamaria, M. Soleymani, E. Jorswieck, and J. Gutiérrez, "Snr maximization in beyond diagonal ris-assisted single and multiple antenna links," *IEEE Signal Processing Letters*, vol. 30, pp. 923–926, 2023. [Online]. Available: https://ieeexplore.ieee.org/document/10187688/

[7] J. C. Gower and G. B. Dijksterhuis, *Procrustes Problems*. OUP Oxford, 2004. [Online]. Available: https://books.google.co.uk/books?id=kRRREAAAQBAJ

[8] T. Bell, "Global positioning system-based attitude determination and the orthogonal procrustes problem," *Journal of Guidance, Control, and Dynamics*, vol. 26, pp. 820–822, 9 2003. [Online]. Available: https://arc.aiaa.org/doi/10.2514/2.5117

[9] G. H. Golub and C. F. V. Loan, *Matrix Computations*. Johns Hopkins University Press, 2013. [Online]. Available: https://jhupbooks.press.jhu.edu/title/matrix-computations

[10] F. Nie, R. Zhang, and X. Li, "A generalized power iteration method for solving quadratic problem on the stiefel manifold," *Science China Information Sciences*, vol. 60, p. 112101, 11 2017. [Online]. Available: http://link.springer.com/10.1007/s11432-016-9021-9

[11] T. Abrudan, J. Eriksson, and V. Koivunen, "Conjugate gradient algorithm for optimization under unitary matrix constraint," *Signal Processing*, vol. 89, pp. 1704–1714, 9 2009. [Online]. Available: https://linkinghub.elsevier.com/retrieve/pii/S0165168409000814

[12] T. E. Abrudan, J. Eriksson, and V. Koivunen, "Steepest descent algorithms for optimization under unitary matrix constraint," *IEEE Transactions on Signal Processing*, vol. 56, pp. 1134–1147, 3 2008. [Online]. Available: http://ieeexplore.ieee.org/document/4436033/

[13] P.-A. Absil, R. Mahony, and R. Sepulchre, *Optimization Algorithms on Matrix Manifolds*. Princeton University Press, 2009. [Online]. Available: https://books.google.co.uk/books?id=NSQGQeLN3NcC

[14] C. Pan, G. Zhou, K. Zhi, S. Hong, T. Wu, Y. Pan, H. Ren, M. D. Renzo, A. L. Swindlehurst, R. Zhang, and A. Y. Zhang, "An overview of signal processing techniques for ris/irs-aided wireless systems," *IEEE Journal of Selected Topics in Signal Processing*, vol. 16, pp. 883–917, 8 2022. [Online]. Available: https://ieeexplore.ieee.org/document/9847080/

[15] D. Semmler, M. Joham, and W. Utschick, "High snr analysis of ris-aided mimo broadcast channels." IEEE, 9 2023, pp. 221–225. [Online]. Available: https://ieeexplore.ieee.org/document/10304487/


[3] Similar conclusion was made for diagonal RIS in [15].